Molecular dynamics simulations of LiCl association and NaCl association in water by means of ABEEM/MM

ARTICLE *in* SCIENCE IN CHINA SERIES B CHEMISTRY · NOVEMBER 2008

Impact Factor: 1.2 · DOI: 10.1007/s11426-008-0129-x

3 AUTHORS, INCLUDING:

Li-Dong Gong
Liaoning Normal University
36 PUBLICATIONS **246** CITATIONS
SEE PROFILE

Zhong-Zhi Yang
Liaoning Normal University
119 PUBLICATIONS **1,432** CITATIONS
SEE PROFILE

Science in China Series B: Chemistry

www.scichina.com
chem.scichina.com
www.springerlink.com

Molecular dynamics simulations of LiCl association and NaCl association in water by means of ABEEM/MM

LI Xin, GONG LiDong & YANG ZhongZhi†

School of Chemistry and Chemical Engeering, Liaoning Normal University, Dalian 116029, China

Constrained molecular dynamics simulations have been used to investigate the LiCl and NaCl ionic association in water in terms of atom-bond electronegativity equalization method fused into molecular mechanics (ABEEM/MM). The simulations make use of the seven-site fluctuating charge and flexible ABEEM-7P water model, based on which an ion-water interaction potential has been constructed. The mean force and the potential of mean force for LiCl and NaCl in water, the charge distributions, as well as the structural and dynamical properties of contact ion pair dissociation have been investigated. The results are reasonable and informative. For LiCl ion pair in water, the solvent-separated ion pair configurations are more stable than contact ion pair configurations. The calculated PMF for NaCl in water indicates that contact ion pair and solvent-separated ion pair configurations are of comparable stability.

atom-bond electronegativity equalization method fused into molecular mechanics (ABEEM/MM), molecular dynamics simulation, ionic association

1 Introduction

It has been recognized for a long time that understanding of many chemical and biological processes requires a deeper knowledge of ionic association because it plays an important role in chemical reactions in solution. A general scheme for the reaction of two ionic solutes may be written as

$$\underset{\text{free ions}}{R^+ + X^-} \Leftrightarrow \underset{\text{SSIP}}{R^+ // X^-} \Leftrightarrow \underset{\text{CIP}}{R^+ / X^-} \Leftrightarrow \underset{\text{product}}{RX}, \quad (1)$$

in which RX is the product of a reaction between the ions R^+ and X^-. The intermediate state, R^+/X^- and $R^+//X^-$, represents a contact ion pair (CIP) and a solvent-separated ion pair (SSIP), respectively. The spectroscopy experiments[1−5] provide some useful information and accurate measurements of the relative populations of CIP and SSIP state. Theoretically, there have been many integral equations[6−10] and computational studies[11−27] of ionic association. Especially, great attention has been paid to the potential of mean force (PMF), $W(r)$, for alkali-halides in aqueous solution. $W(r)$ can be obtained from different methods. On one hand, $W(r)$ can be obtained from the solute-solute radial distribution function, $g(r)$, by using $W(r) = -k_B T \ln g(r)$. On the other hand, $W(r)$ may be obtained by integration of the mean force, $F(r)$, between solute particles by using $F(r) = -\frac{\mathrm{d}}{\mathrm{d}r} W(r)$, and $F(r)$ can be determined during the constrained molecular dynamics simulations[15] of the system, i.e., an additional constraint on the solute particles at fixed separations.

In the present work, we use the constrained molecular dynamics simulations in terms of the ABEEM-7P water model[28−31] to calculate the mean force and the PMF for the LiCl and NaCl ion pairs. The present simulations differ from previous treatments in the following respects. First, the ABEEM-7P water model used here can give accurate description for a flexible water molecule with seven-site fluctuating charge, corresponding to a more

Received May 30, 2008; accepted July 20, 2008
doi: 10.1007/s11426-008-0129-x
†Corresponding author (email: zzyang@lnnu.edu.cn)
Supported by the National Natural Science Foundation of China (Grant Nos. 20633050 and 20703022)

realistic model of aqueous electrolyte solutions. Second, the ABEEM/MM-based ion-water interaction potential[32−34] has been constructed by gas-phase clusters and effectively transferred to aqueous ionic solutions, and hence, experimental gas-phase data can be incorporated into the development of reliable ion-water interaction model. Third, the constrained molecular dynamics simulation allows determining the average structure of the solvent around the ions for each separation without the need of complementary simulations.

2 Method

Based on the density functional theory (DFT), the electronegativity equalization method (EEM) has been parameterized and validated for atomic charges calculations by Geerlings et al.[35,36]. Moreover, EEM has been successfully applied to molecular mechanics (MM) and molecular dynamics (MD) simulation by Chelli et al.[37] and Smirnov et al.[38]. The atom-bond electronegativity equalization method (ABEEM) has been designed and applied successfully to calculating the energy, charge distribution, etc., of a large organic or biological molecule[39−42]. Recently, ABEEM has been fused into MM, i.e., ABEEM/MM, which has been applied to the water and ion/water systems[28−34]. The total energy of a system consisting of an ion pair and many water molecules is given in Eq. (2) based on ABEEM/MM,

$$
\begin{aligned}
E = & \sum_{\text{bonds}} D[e^{-2\alpha(r-r_{eq})} - 2e^{-\alpha(r-r_{eq})}] + \sum_{\text{angles}} f_\theta(\theta-\theta_{eq})^2 + \sum_i \sum_j 4\varepsilon_{ij}\left[\left(\frac{\sigma_{ij}}{r_{ij}}\right)^{12} - \left(\frac{\sigma_{ij}}{r_{ij}}\right)^{6}\right] \\
& + \sum_{i=1}^{N_{mol}} \left\{ \sum_{j=1(\neq i)}^{N_{mol}} \left[\sum_{\substack{H\in i \\ (H,lp \text{ in } HBIR)}} \sum_{lp\in j} k_{lp,H}(r_{iH,j(lp)}) \frac{q_{iH} q_{j(lp)}}{r_{iH,j(lp)}} + \left(\frac{1}{2} \sum_a \sum_b \frac{q_{ia} q_{jb}}{r_{ia,jb}} \right.\right.\right. \\
& + \frac{1}{2} \sum_{a-b} \sum_{g-h} \frac{q_{i(a-b)} q_{j(g-h)}}{r_{i(a-b),j(g-h)}} + \frac{1}{2} \sum_{lp} \sum_{lp'} \frac{q_{i(lp)} q_{j(lp')}}{r_{i(lp),j(lp')}} \\
& \left.\left.\left. + \sum_{g-h} \sum_a \frac{q_{ia} q_{j(g-h)}}{r_{ia,j(g-h)}} + \sum_{\substack{a\neq H, H \text{ in } HBIR \\ \text{and } lp \text{ not in } HBIR)}} \sum_{a} \sum_{lp} \frac{q_{ia} q_{j(lp)}}{r_{ia,j(lp)}} + \sum_{lp} \sum_{a-b} \frac{q_{i(a-b)} q_{j(lp)}}{r_{i(a-b),j(lp)}} \right) \right] \right. \\
& + \left[\sum_{lp(\text{in}HI)} k_{R^+,i(lp)} \frac{q_{R^+} q_{i(lp)}}{r_{R^+,i(lp)}} + \left(\sum_a \frac{q_{R^+} q_{ia}}{r_{R^+,ia}} + \sum_{a-b} \frac{q_{R^+} q_{i(a-b)}}{r_{R^+,i(a-b)}} + \sum_{lp(\text{not in}HI)} \frac{q_{R^+} q_{i(lp)}}{r_{R^+,i(lp)}} \right) \right] \\
& \left. + \left[\sum_H k_{X^-,iH}(r_{X^-,iH}) \frac{q_{X^-} q_{iH}}{r_{X^-,iH}} + \left(\sum_{a(\neq H)} \frac{q_{X^-} q_{ia}}{r_{X^-,ia}} + \sum_{a-b} \frac{q_{X^-} q_{i(a-b)}}{r_{X^-,i(a-b)}} + \sum_{lp} \frac{q_{X^-} q_{i(lp)}}{r_{X^-,i(lp)}} \right) \right] \right\} + \frac{q_{R^+} q_{X^-}}{r_{R^+,X^-}},
\end{aligned}
\tag{2}
$$

where the first and second terms stand for the energy of O—H bond stretching in the form of the Morse potential and H—O—H angle bending in the form of harmonic potential, respectively, accounting for the intramolecular vibration of water molecule. Here, the bond dissociation energy D is 529.6 kcal·mol^{-1}(1 cal = 4.184 J), and the angle force constant f_θ is 34.05 kcal·mol^{-1}·deg^{-2}. r_{eq} and θ_{eq} denote the equilibrium values of the bond length and bond angle, and r and θ stand for the actual values of bond lengths and bond angles, respectively. The third term of eq. (2) represents the van der Waals interactions, in which the Lennard-Jones 12-6 potential is employed, ε_{ij} and σ_{ij} are the Lennard-Jones parameters, and r_{ij} is the distance between atoms i and j. The coulombic expression is used to describe the electrostatic interaction of the system. The fourth term includes the electrostatic interaction between water molecules, cation-water interaction, and anion-water interactions. In the ABEEM-7p water model, the electrostatic interaction sites of H_2O are represented by seven sites, i.e., three atoms, two O—H bonds and two lone-pair electrons of O. q is the ABEEM charge, the subscripts a and b denote atoms, $a-b$ and $g-h$ denote O—H bonds, lp denotes the lone-pair electrons of O, i and j denote H_2O molecules, and R^+ and X^- denote the cation and anion of the ion pair, respectively. q_{ia} and $q_{i(a-b)}$ are the ABEEM

charges on atom a and bond $a-b$ in water molecule i, respectively. The bond charge is located on the point that partitions the bond length according to the ratio of covalent atomic radii of two bonded atoms. $r_{ia,jb}$ is the distance between atom a in water molecule i and atom b in water molecule j, respectively. The cation-anion interaction includes a Lennard-Jones term plus coulombic contribution. The electrostatic interactions between all charge sites are calculated using ABEEM charges[39−42]. The ABEEM/MM parameters have been tested in water and ion/water clusters as well as in liquid water and aqueous ionic solutions[28−34], for example, the optimized parameter $k_{R^+,i(lp)}$ is 0.96 for alkali metal cations, $k_{\mathrm{Cl,H}}(r_{\mathrm{Cl,H}}) = 1.000 - \frac{0.124}{1+e^{(r_{\mathrm{Cl,H}}-2.341)/0.119}}$, and so on. The ABEEM/MM parameters are summarized in Table 1.

Table 1 ABEEM and van der Waals parameters

Atom type	ABEEM parameters[a]				van der Waals parameters	
	χ^{*}[b]	$2\eta^{*}$	C	D	σ(Å)	E (kcal·mol^{-1})
H−	2.023	3.774	2.161		2.240	0.012
O−	3.773	26.098	11.493	5.312	3.051	0.044
H−O	5.136	24.767	2.161	11.493		
*lp*O−	3.308	6.692	5.312			
Li^+	9.402	45.030			1.506	0.166
Na^+	7.050	40.039			2.350	0.130
Cl^-					3.578	0.100

a) The ABEEM parameters are employed to compute the ABEEM charges. χ^{*} denotes the valence-state electronegativity, $2\eta^{*}$ the valence-state hardness, and C and D denote adjustable parameters; b) The Pauling electronegativity scaling unit is used.

In this work, we consider a system composed of two solutes, R^+ and X^- (R^+=Li^+ or Na^+ and X^-=Cl^-), with 214 water molecules. Molecular dynamics simulations of the system are performed keeping the LiCl separation and the NaCl separation fixed[15]. The mean force between the two solutes ($F(r)$) can be written as

$$F(r) = F_d(r) + \Delta F(r), \tag{3}$$

where $F_d(r)$ is the direct solute-solute force, and $\Delta F(r)$ is solvent contribution to the solute-solute mean force. Thus, the PMF, $W(r)$, can be calculated by integrating

$$W(r) = W(r_0) - \int_{r_0}^{r} F(r)\mathrm{d}r. \tag{4}$$

$W(r_0)$ should be chosen to obtain the reliable PMF at long separations. In general, $W(r_0)$ should coincide with the macroscopic Coulomb potential, $W(r_0) = \frac{q_{R^+}q_{X^-}}{\varepsilon r_0}$, where q_{R^+} and q_{X^-} are the ionic charges, and ε is the ABEEM-7P water dielectric constant[28,29]. Note that we take r_0=7.0 Å for LiCl ion pair and r_0=8.0 Å for NaCl ion pair, respectively. The constrained molecular dynamics simulations were carried out in a cubic box with periodic boundary condition and minimum image convention. The side length was 18.625 Å and the temperature of the system was kept at 298 K by Berendsen algorithm[43]. The equations of motion were solved using the velocity Verlet algorithm. The nonbonded interactions were truncated using the force shifting[44] at a molecular separation of 9.0 Å for all simulations, making the calculated forces and energy smoothly shift to zero at the cutoff distance.

3 Results and discussion

3.1 The PMF

The free energy of the ion pair as a function of ionic separation is known as the PMF, and its form reveals many interesting details about the solvation of ionic species in solution and is relevant to many characteristics of ionic reactions. We have calculated the PMFs for the LiCl and NaCl ion pairs in ABEEM-7P water using the standard integration technique in constrained molecular dynamics simulations. At each step in the calculations, the ion-pair separation was fixed and the average force along the ion-pair axis was calculated as a function of distance, then the average force was subsequently integrated to give the PMF. For these calculations, the ion-pair separations have been fixed at distances between 2.0 and 7.0 Å for the LiCl ion pair, and between 2.5 and 8.0 Å for the NaCl ion pair, with both having a separation increment of 0.25 Å. The total simulation time at each ion-pair separation was at least 200 ps, and substantially longer averaging was performed in the important regions such as the region of CIP and its dissociation barrier. Figure 1 displays the PMFs of LiCl and NaCl in ABEEM-7P water. They are undulate but not monotonic curves.

Table 2 contains a summary of the average forces for all separations of the LiCl and NaCl ion pairs. The barriers for LiCl ionic dissociation and association are 2.05

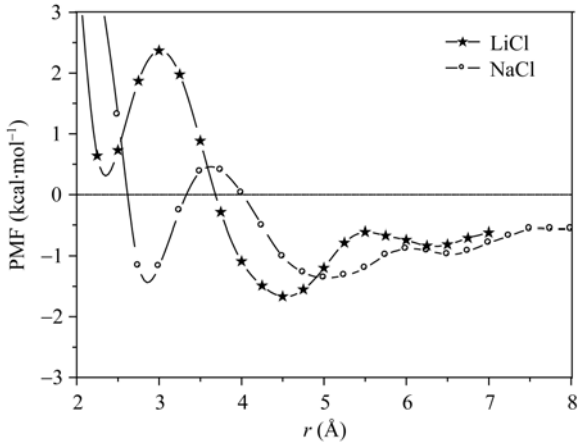

Figure 1 The PMFs of LiCl and NaCl in ABEEM-7P water

Table 2 Average forces for different separations of the LiCl and NaCl ion pairs[a)]

LiCl		NaCl	
Distance (Å)	Ave. force (kcal·mol^{-1}·Å^{-1})	Distance (Å)	Ave. force (kcal·mol^{-1}·Å^{-1})
2.00	18.9	2.50	16.1
2.25	1.9	2.75	3.7
2.50	–3.5	3.00	–3.7
2.75	–3.2	3.25	–3.5
3.00	–0.4	3.50	–1.6
3.25	1.1	3.75	1.4
3.50	1.4	4.00	1.6
3.75	2.4	4.25	2.7
4.00	1.3	4.50	1.3
4.25	0.8	4.75	0.8
4.50	0.0	5.00	–0.1
4.75	–0.2	5.25	–0.2
5.00	–0.7	5.50	–0.8
5.25	–0.8	5.75	–0.9
5.50	0.1	6.00	0.1
5.75	–0.1	6.25	0.1
6.00	0.4	6.50	0.4
6.25	–0.3	6.75	–0.8
6.50	–0.5	7.00	–0.3
6.75	–0.6	7.25	–0.6
7.00	–0.4	7.50	–0.3
		7.75	0.3
		8.00	–0.3

a) The largest uncertainty of mean force in the simulations is 0.2 kcal·mol^{-1}·Å^{-1}.

and 4.04 kcal/mol, respectively. Recently, Zhang and Duan[25] reported that the barriers for LiCl ionic dissociation and association are 1.60 and 5.68 kcal/mol, respectively, and the population of ion pair in SSIP state is much larger than that of CIP. The present study shows that the barrier for LiCl ionic association is higher than that for ionic dissociation, the solvent-separated region is significantly broader than the contact region, and SSIP configurations are more stable than CIP configurations. This is consistent with the results of Zhang and Duan.

The barrier for NaCl dissociation is 1.83 kcal/mol and the association barrier is 1.76 kcal/mol. There is a comparable stability for the CIP and SSIP configurations in the NaCl solution. This is also consistent with the results of Smith and Dang[16], who reported that the barrier to CIP dissociation is 1.8 kcal/mol, and the SSIP minimum is 0.2 kcal/mol less stable than the CIP minimum. They also pointed out that previous calculations[17] of the PMF of NaCl have varied substantially in the predictions of the relative stability of CIP and SSIP configurations, in part, due to variations in both the ion-water and water-water interactions employed.

3.2 Structures

Several structural properties of the ionic association process have been investigated, and the barrier region between the CIP and SSIP configurations is the focus. The LiCl ion-pair separation fixed at 3.0 Å and the NaCl ion-pair separation fixed at 3.75 Å need longer calculations, and their configurations are very near to the peaks in the PMFs shown in Figure 1. Orientational correlation functions for water molecules in the first solvation shell of the ions in LiCl and NaCl solutions are displayed in Figure 2. A water molecule is defined as being coordinated to the lithium ion if $r_{\text{Li-O}} \leqslant 2.84$ Å, to the sodium ion if $r_{\text{Na-O}} \leqslant 3.20$ Å, and to the chloride ion if $r_{\text{Cl-H}} \leqslant 2.80$ Å. Bridging water molecules are coordinated to both ions simultaneously. The orientation of the water molecules is defined in terms of the angle between the ion-oxygen vector and the water HOH bisector. It is evident from Figure 2 that bridging water molecules have substantially perturbed the orientations compared with singly coordinated molecules, i.e., there are strained solvent configurations around the barrier region.

The use of a flexible water model allows us to discuss the intramolecular geometry of the water molecules. The presence of cation and anion leads to a certain distortion of the surrounding water molecules. Here, we take three types of water molecules into account: the singly coordinated water molecules in the first solvation shell of

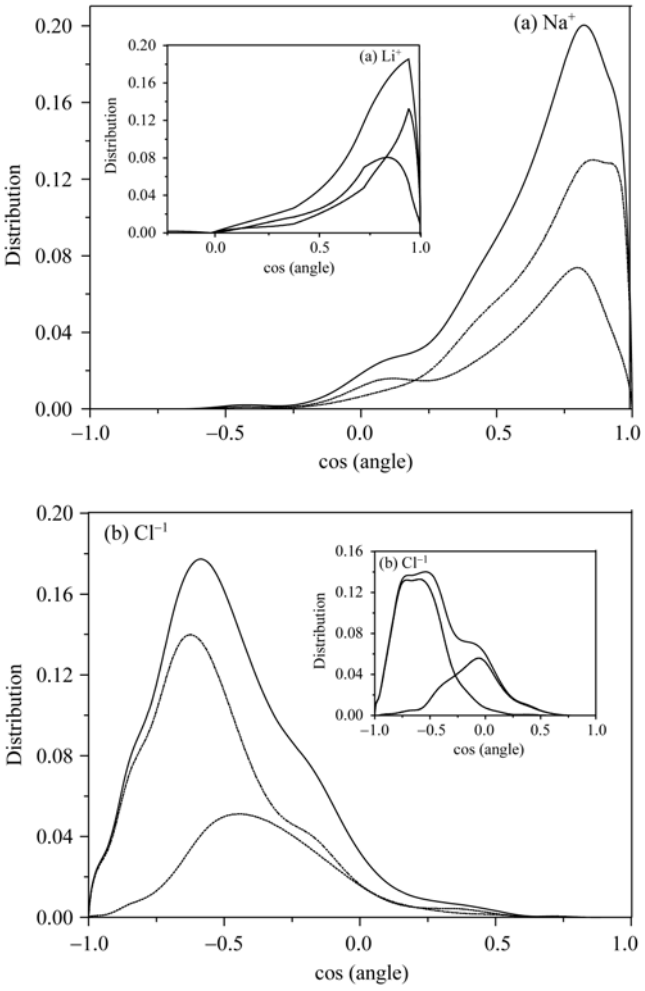

Figure 2 First solvation shell orientational correlation functions around Li^+ and Na^+ (a), and Cl^- in LiCl and NaCl (b) solutions. The first solvation shell water molecules are represented with solid line. Bridging water molecules are represented with short dash line. Singly coordinated water molecules in the first sovlation shell are represented with dash dotted line.

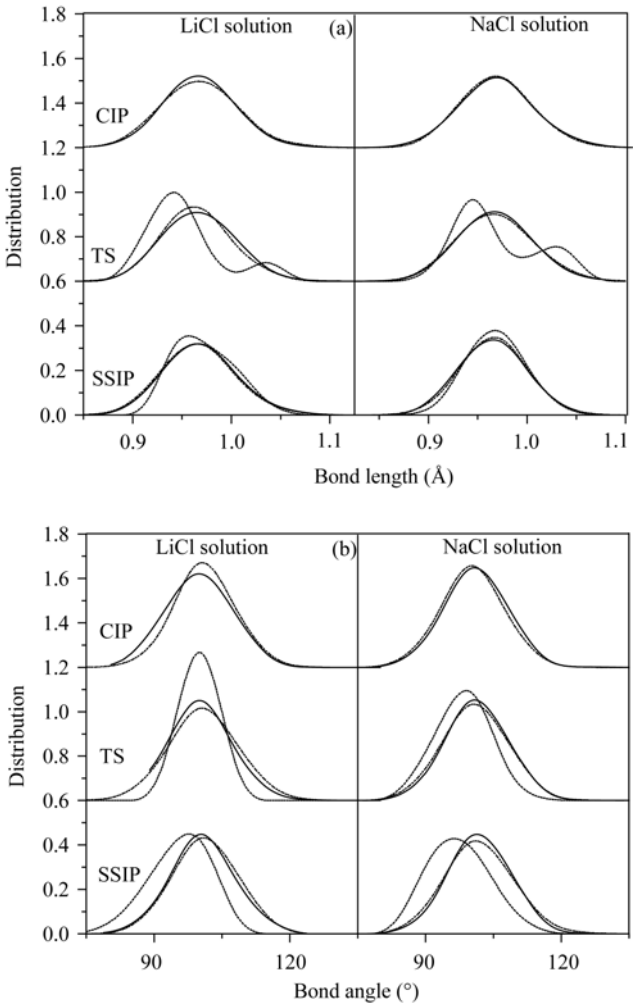

Figure 3 The distributions of the bond length (a) and the bond angle (b) of the water molecules in the first solvation shells of ions in LiCl and NaCl solutions for different interionic separations. Singly coordinated water molecules in the first solvation shell of Li^+ or Na^+ are represented with solid line. Bridging water molecules are represented with short dash line. Singly coordinated water molecules in the first solvation shell of Cl^- are represented with dash dotted line.

cation (Li^+ or Na^+), the singly coordinated water molecules in the first shell of Cl^-, and the bridging water molecules. The distributions of the bond length and the bond angle of the three types of water molecules in LiCl and NaCl solutions are displayed in Figure 3. Compared to an isolated water molecule, the OH bonds of bound water molecules are elongated and the closing of the HOH angle is also observed in the simulations because of the environment.

As shown in Figure 3, the distributions of bond length and bond angle of the bridging water molecules are distinctive in LiCl and NaCl solutions. For the distribution of the bond length in the transition state (TS) configurations, there are two peaks: one is higher and shifts to shorter distances and the other is lower and shifts to longer distances, which demonstrates that there are two types of OH bonds (the bound and the free ones) for the bridging water molecules. However, in SSIP configurations, the two peaks have merged because the bridging water molecules have perfectly separated the ion pair. For the distribution of the bond angle of the bridging water molecules, the peak shifts to smaller angles from TS to SSIP configurations. Moreover, because the common picture from CIP to SSIP interconversion process involves considerable solvent reorganization around the ion pair, we have analyzed the solvent structure around the ion pair for the three ionic separations that correspond to 2.25 Å (CIP), 3.00 Å (TS) and 4.5 Å

(SSIP) for the lithium chloride ion pair, and correspond to 3.0 Å (CIP), 3.75 Å (TS) and 5.0 Å (SSIP) for the sodium chloride ion pair. We have calculated the mean number densities of oxygen and hydrogen atoms in the plane that contains the interionic axis. The contour lines for densities of oxygen and hydrogen atoms are shown in Figure 4, which gives more clear pictures of densities of oxygen and hydrogen atoms in one figure. In doing so, the positions and orientations of the water molecules around the ion pair can be identified. Obviously, for the chloride ion, the figure indicates the formation of a first hydration shell of hydrogen atoms, while for the cations (Li^+ and Na^+), the figure displays the formation of a first hydration shell of oxygen atoms. In addition, as shown in Figure 4, from the solvent distribution in the CIP region to that in the SSIP region, the water molecules are inserting themselves into the ions step by step, and finally they are located between the ions in the SSIP region.

3.3 ABEEM charges

A significant feature of our model consists in giving the charge distribution of the whole system. Tables 3 and 4 show the ABEEM charges of the bridging water molecules, the singly coordinated water molecules around Li^+ or Na^+ and Cl^- in the LiCl and NaCl solutions respectively.

For both solutions, the positive charges are located on the cations, the oxygen atom and the hydrogen atom, and at the same time, the negative charges are located on the chloride ion, the oxygen-hydrogen bond and the lone pair. Moreover, in different ionic separations, the charges of the hydrogen atom and the lone pair are special because the hydrogen atom is toward the anion and the

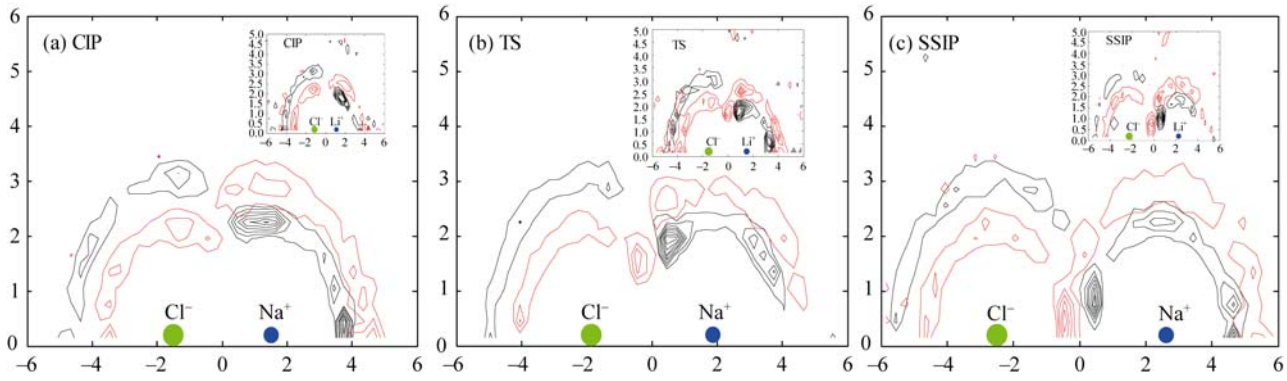

Figure 4 Contour line of the oxygen (solid line) and hydrogen (short dash line) density profile around the LiCl ion pair and the NaCl ion pair for different interionic separations. (a) CIP; (b) TS; (c) SSIP.

Table 3 The average ABEEM charges for the bridging water molecules and the singly coordinated water molecules around Li^+ and Cl^- in the LiCl solution

	O atom	H atom	OH bond	Lone pair
CIP				
Water (Li^+)	0.105±0.024	0.368±0.118	–0.147±0.013	–0.280±0.077
Water (Cl^-)	0.102±0.006	0.352±0.061	–0.145±0.005	–0.254±0.033
TS				
Bridging water	0.096±0.006	0.306±0.070	–0.145±0.003	–0.209±0.051
Water (Li^+)	0.102±0.018	0.353±0.116	–0.146±0.011	–0.256±0.080
Water (Cl^-)	0.100±0.007	0.334±0.073	–0.145±0.006	–0.236±0.035
SSIP				
Bridging water	0.086±0.019	0.428±0.115	–0.135±0.011	–0.232±0.053
Water (Li^+)	0.104±0.023	0.343±0.115	–0.148±0.012	–0.260±0.083
Water (Cl^-)	0.100±0.008	0.336±0.066	–0.145±0.006	–0.235±0.033

Table 4 The average ABEEM charges for the bridging water molecules and the singly coordinated water molecules around Na^+ and Cl^- in the NaCl solution

	O atom	H atom	OH bond	Lone pair
CIP				
Water (Na^+)	0.104±0.016	0.335±0.091	–0.148±0.009	–0.255±0.050
Water (Cl^-)	0.101±0.009	0.352±0.066	–0.145±0.006	–0.247±0.033
TS				
Bridging water	0.100±0.012	0.377±0.081	–0.142±0.007	–0.245±0.049
Water (Na^+)	0.105±0.017	0.332±0.096	–0.148±0.010	–0.258±0.055
Water (Cl^-)	0.100±0.012	0.352±0.086	–0.144±0.008	–0.240±0.040
SSIP				
Bridging water	0.084±0.021	0.429±0.087	–0.135±0.012	–0.225±0.062
Water (Na^+)	0.104±0.027	0.352±0.137	–0.148±0.015	–0.264±0.074
Water (Cl^-)	0.101±0.006	0.338±0.063	–0.145±0.005	–0.241±0.034

lone pair orients to the cation. In the LiCl solution, the polarization influence of the lithium ion is stronger than that of the chloride ion, therefore, the absolute values of the positive charge of the hydrogen atom and the negative charge of the lone pair on the singly coordinated water molecules around Li^+ are higher than those around Cl^-, i.e., the Li^+-water interaction is stronger than the Cl^--water hydrogen bond interaction. Moreover, the hydrogen atoms of the bridging water molecules have larger charges in SSIP configurations than in TS configurations because the water molecules have strong interactions with both the cation and the anion in the SSIP state. In the NaCl solution, the positive charges of the hydrogen atoms of the singly coordinated water molecules around Cl^- are calculated to be higher than those around Na^+ in the CIP and TS state. Although it is not the case for the SSIP state, there is a larger hydrogen charge fluctuation for the water molecules around Na^+ ($\pm$0.137) than that around Cl^- ($\pm$0.063) in this state. The negative charges of the lone pairs of the singly coordinated water molecules around Na^+ are lower than those around Cl^-. The polarization influence of Na^+ only makes the adjacent lone pairs have more negative charges, but it cannot make the hydrogen atoms of singly coordinated water molecules have more positive charges. The polarization effect of Cl^- makes the coordinated hydrogen atoms have more positive charges. In addition, the charges of the hydrogen atoms of the bridging water molecules are larger than those of singly coordinated water molecules in the TS state, and they are more positive in the SSIP state, because water molecules have stronger and stronger interactions with the ions when they change from free molecules to bridging molecules.

The charge distributions of the hydrogen atoms and the lone pairs of the water molecules in the first solvation shells of ions shown in Figure 5 can provide some information of the ionic association process. First, the charges of the hydrogen atoms and the lone pairs of the singly coordinated molecules around the cation have wider distributions than those around the anion. Second, the hydrogen charge distribution of the bridging water molecules has two peaks in the TS and SSIP configurations in both solutions, which gives two kinds of hydrogen atoms (the bound and the free ones). Moreover, the shape of peak is different between the TS state and the SSIP state, and it is also different between the LiCl solution and the NaCl solution. In the LiCl solution, the higher peak (the hydrogen atom has small positive charge) in the TS state has changed into the lower peak in the SSIP state, and the lower peak (the hydrogen atom has large positive charge) in the TS state has changed into the higher peak in the SSIP state. In the NaCl solution, the changed shape of peak is not very obvious, but can be seen: the lower peak in the TS state has changed into the higher peak in the SSIP state, and the higher peak in the TS state has changed into the lower peak in the SSIP state. These changes reflect the different environments such as the different configurations (TS and SSIP) and the different solutions (LiCl and NaCl solu-

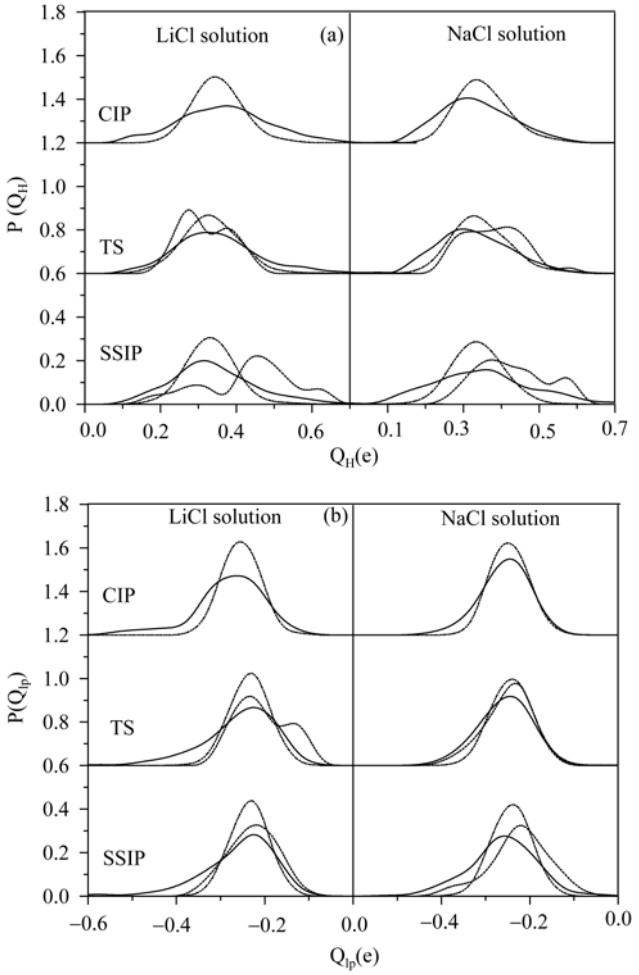

Figure 5 The ABEEM charge distributions of the hydrogen atom (a) and the lone pair of the water molecules (b) in the first solvation shell of ions in LiCl and NaCl solutions for different interionic separations. Singly coordinated water molecules in the first solvation shell of Li^+ or Na^+ are represented with solid line. Bridging water molecules are represented with short dash line. Singly coordinated water molecules in the first solvation shell of Cl^- are represented with dash dotted line.

tions) that have distinct electrostatic fields formed by the ions and the water dipole. Third, the charge distribution of the lone pair also has two peaks in TS configurations in the LiCl solution, but this phenomenon cannot be observed in the NaCl solution, because Na^+ can have equivalent interactions with the two lone pairs of a bridging water molecule; however, Li^+ is much smaller than Na^+, and can only have stronger interaction with one lone pair. So in TS configuration, there exist two types of lone-pair electrons of water molecule directly coordinated around the Li^+ in LiCl solution, while there is only one type in NaCl solution. All in all, the charge distributions of the hydrogen atoms and the lone pairs can reveal two types of hydrogen atoms of the bridging water molecules in both solutions and two types of lone pairs of the bridging water molecules in TS configurations in the LiCl solution. In other words, the fluctuating charge model is sensitive to the configuration of system and can readjust timely the changed electrostatic field.

3.4 CIP dissociation dynamics

The dynamics of interconversion of CIP and SSIP configurations is very important to the kinetics of ion-pair reactions in solutions. Classical transition state theory (TST) predicts that the rate constant for CIP dissociation is a function of the temperature as well as the ion-pair reduced mass and the PMF in the CIP region. The TST forward rate constant for this reaction is given explicitly by[45]

$$k_f^{TST} = (2\pi\beta\mu_I)^{-1/2} \frac{(r^{\#})^2 e^{-\beta W(r^{\#})}}{\int_0^{r^{\#}} \mathrm{d}r r^2 e^{-\beta W(r)}}, \quad (5)$$

where $r^{\#}$ is the position of the barrier maximum, $\beta = (k_B T)^{-1}$, and μ_I is the ion pair reduced mass. Taking account of dynamical correction to k_f^{TST}, we can obtain the rate constant $k = \kappa k_f^{TST}$, where κ is the transmission coefficient. The transmission coefficient can be obtained using the method of reactive flux, and the normalized reactive flux can be computed as[46]

$$k(t) = \frac{\left\langle \dot{r}(0)\theta[r(t) - r^{\#}] \right\rangle_c}{\left\langle \dot{r}(0)\theta[\dot{r}(0)] \right\rangle_c}, \quad (6)$$

where $\theta[x]$ is the Heaviside step function. $\theta[x]$ is 1 in case that x is larger than 0, and otherwise $\theta[x]$ is 0. The averages have been computed by starting several trajectories from equilibrated configurations (1000 stored configurations) with the ion pair distance constrained at $r^{\#}$ ($r^{\#}$=3.0 Å for the LiCl ion pair and $r^{\#}$=3.75 Å for the NaCl ion pair), as indicated by the subscript c. Then the constraint is removed, new velocities are sampled from a Boltzmann distribution, and the motion is traced both forward (1.5 ps) and backward (1.5 ps) in time. The normalized reactive flux is shown in Figure 6.

The calculated TST rate constants (k_f^{TST}) are 0.44 and 0.33 ps^{-1} for LiCl and NaCl ion pairs in ABEEM-7P water, respectively, the transmission coefficients (κ) obtained from the plateau value of the normalized reactive flux are 0.26 and 0.37 for LiCl and NaCl pairs in water, respectively, and the corresponding rate constants ($k = \kappa k_f^{TST}$) are 0.11 and 0.12 ps^{-1} for the two pairs in

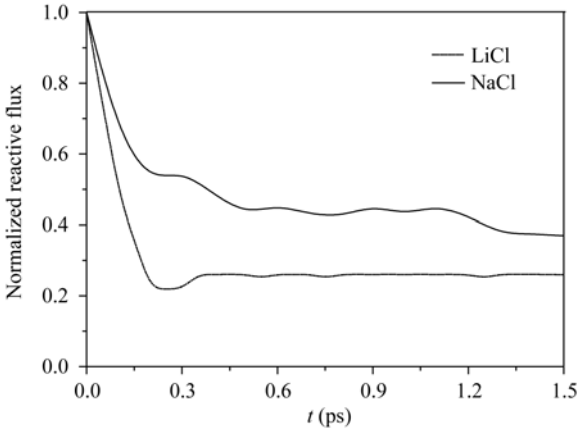

Figure 6 Normalized reactive flux.

water, respectively. We can see that the solvent coupling reduces the rate constant for dissociation to some extent. For the association-dissociation process that takes place between contact and solvent-separated ion pairs for aqueous NaCl solution, Rey et al.[17] reported that TST rate constant was 0.37 ps^{-1}, and the transmission coefficients were 0.22 obtained from the method of reactive flux, 0.22 and 0.37 from the Grote-Hynes theory, and 0.08 and 0.35 from the Kramers theory. There is a little difference between our results and the previous reported results[16−20] in that these results are quite sensitive to the details of PMFs, various approaches for the calculation of transmission coefficient and the potential models used in simulations.

4 Conclusions

We have carried out constrained molecular dynamics simulations on the LiCl association and NaCl ionic association in water by means of ABEEM/MM. For LiCl ion pair in water, the solvent-separated ion pair configurations are more stable than contact ion pair configurations, which is associated with the flexible body and fluctuating charges of the water molecules. The calculated PMF for NaCl in water indicates that contact ion pair and solvent-separated ion pair configurations are of comparable stability. An investigation of the dynamics of contact ion-pair dissociation using the reactive flux method indicates that the solvent coupling reduces the rate constant for dissociation to a certain extent. The present potential model can give the charge distribution of the system responding to the changed electrostatic field, thus it can describe the interactions more properly and can give reliable results. In one word, the ABEEM/MM-based potential simulations may provide more information for the ionic association process and can effectively describe the ionic association reaction.

The authors greatly thank Prof. Jay William Ponder for providing the Tinker program.

1 Simon J D, Peters K S. Picosecond studies of organic photoreactions. Acc Chem Res, 1984, 17: 277−283
2 Spears K G, Gray T H, Huang D. Ionic photodissociation and picosecond solvation dynamics of contact ion pairs. J Phys Chem, 1986, 90: 779−790
3 Spohn P D, Brill T B. Raman spectroscopy of the species in concentrated aqueous solutions of zinc nitrate, calcium nitrate, cadmium nitrate, lithium nitrate and sodium nitrate up to 450 degree C and 30 Mpa. J Phys Chem, 1989, 93: 6224−6231
4 Fleissner G, Hallbrucker A, Mayer E. Increasing contact ion pairing in the supercooled and glassy states of "dilute" aqueous magnesium, calcium, and strontium nitrate solution: Implications for biomolecules. J Phys Chem, 1993, 97: 4806−4814
5 Simonet V, Calzavara Y, Hazemann J L, Argoud R, Geaymond O, Raoux D. X-ray absorption spectroscopy studies of ionic association in aqueous solutions of zinc bromide from normal to critical conditions. J Chem Phys, 2002, 117: 2771−2781
6 Carnie S L, Patey G N. Fluids of polarizable hard spheres with dipoles and tetrahedral quadrupoles integral equation results with application to liquid water. Mol Phys, 1982, 47: 1129−1151
7 Pettitt B M, Rossky P J. Alkali halides in water: Ion-solvent correlations and ion-ion potentials of mean force at infinite dilution. J Chem Phys, 1986, 84: 5836−5844
8 Morita T, Ladanyi B M, Hynes J T. Polar solvent contributions to activation parameters for model ionic reactions. J Phys Chem, 1989, 93: 1386−1392
9 Hummer G, Soumpasis D M. An extended RISM study of simple electrolytes: pair correlations in a NaCl-SPC water model. Mol Phys, 1992, 75: 633−651
10 Kovalenko A, Hirata F. Potentials of mean force of simple ions in ambient aqueous solution. I. Three-dimensional reference interaction site model approach. J Chem Phys, 2000, 112: 10391−10402
11 Belch A C, Berkowitz M, McCammon J A. Solvation structure of a sodium chloride ion pair in water. J Am Chem Soc, 1986, 108: 1755−1761
12 Karim O A, McCammon J A. Dynamics of a sodium chloride ion pair in water. J Am Chem Soc, 1986, 108: 1762−1766
13 Jorgensen W L, Buckner J K, Houston S E, Rossky P J. Hydration and energetics for $(CH_3)_3CCl$ ion pairs in aqueous solution. J Am Chem Soc, 1987, 109: 1891−1899
14 Buckner J K, Jorgensen W L. Energetics and hydration of the constituent ion pairs of tetramethylammonium chloride. J Am Chem Soc,

1989, 111: 2507－2516
15 Ciccotti G, Ferrario M, Hynes J T, Kapral R. Dynamics of ion pair interconversion in a polar solvent. J Chem Phys, 1990, 93: 7137－7147
16 Smith D E, Dang L X. Computer simulations of NaCl association in polarizable water. J Chem Phys, 1994, 100: 3757－3766
17 Rey R, Guàrdia E. Dynamical aspects of the Na^+-Cl^- ion pair association in water. J Phys Chem, 1992, 96: 4712—4718
18 Dang L X, Rice J E, Kollmann P A. The effect of water models on the interaction of the sodium-chloride ion pair in water: Molecular dynamics simulations. J Chem Phys, 1990, 93: 7528—7529
19 Smith D E, Haymet A D J. Structure and dynamics of water and aqueous solutions: The role of flexibility. J Chem Phys, 1992, 96: 8450—8459
20 Berkowitz M, Karim O A, McCammon J A, Rossky P J. Sodium chloride ion pair interaction in water: Computer simulation. Chem Phys Lett, 1984, 105: 577－580
21 Zhu S -B, Robinson G W. Molecular-dynamics computer simulation of simulation of an aqueous NaCl solution: Structure. J Chem Phys, 1992, 97: 4336－4348
22 Bader J S, Chandler D. Computer simulation study of the mean forces between ferrous and ferric ions in water. J Phys Chem, 1992, 96: 6423－6427
23 Chialvo A A, Cummings P T, Cochran H D, Simonson J M, Mesmer R E. Na^+-Cl^- ion pair association in supercritical water. J Chem Phys, 1995, 103: 9379－9387
24 Shinto H, Morisada S, Miyahara M, Higashitani K. A reexamination of mean force potentials for the methane pair and the constituent ion pairs of NaCl in water. J Chem Eng Jpn, 2003, 36: 57－65
25 Zhang Z G, Duan Z H. Lithium Chloride ionic association in dilute aqueous solution: A constrained molecular dynamics study. Chem Phys, 2004, 297: 221－233
26 Torrie G M, Valleau J P. Nonphysical sampling distributions in Monte Carlo free-energy estimation: Umbrella sampling. J Comput Phys, 1977, 23: 187－199
27 Pangali C, Rao M, Berne B J. A Monte Carlo simulation of the hydrophobic interaction. J Chem Phys, 1979, 71: 2975－2981
28 Yang Z Z, Wu Y, Zhao D X. Atom-bond electronegativity equalization method fused into molecular mechanics. I. A seven-site fluctuating charge and flexible body water potential function for water clusters. J Chem Phys, 2004, 120: 2541－2557
29 Wu Y, Yang Z Z. Atom-bond electronegativity equalization method fused into molecular mechanics. II. A seven-site fluctuating charge and flexible body water potential function for liquid water. J Phys Chem A, 2004, 108: 7563－7576
30 Yang Z Z, Qian P. A study of *N*-methylacetamide in water cluster: Based on atom-bond electronegativity equalization method fuse into molecular mechanics. J Chem Phys, 2006, 125(6): 064311－064326
31 Qian P, Yang Z Z. Application of ABEEM/MM model to study the properties of the water clusters $(H_2O)_n$, n=7－10. Sci Chin Ser B-Chem, 2007, 50: 190－204
32 Li X, Yang Z Z. Study of lithium cation in water clusters: Based on atom-bond electronegativity equalization method fused into molecular mechanics. J Phys Chem A, 2005, 109: 4102－4111
33 Li X, Yang Z Z. Hydration of Li^+-ion in atom-bond electronegativity equalization method–7p water: A molecular dynamics simulation study. J Chem Phys, 2005, 122: 084514－084528
34 Yang Z Z, Li X. Ion solvation in water from molecular dynamics simulation from the ABEEM/MM force field. J Phys Chem A, 2005, 109: 3517－3520
35 Bultinck P, Langenaeker W, Lahorte P, Proft F D, Geerlings P, Waroquier M, Tollenaere J P. The electronegativity equalization method I: Parameterization and validation for atomic charge calculations. J Phys Chem A, 2002, 106: 7887－7894
36 Bultinck P, Langenaeker W, Lahorte P, Proft F D, Geerlings P, Alsenoy C V, Tollenaere J P. The electronegativity equalization method II: Application of different atomic charge schemes. J Phys Chem A, 2002, 106: 7895－7901
37 Chelli R, Procacci P. A transferable polarizable electrostatic force field for molecular mechanics based on the chemical potential equalization principle. J Chem Phys, 2002, 117: 9175－9181
38 Smirnov K S, van de Graaf B. Consistent implementation of the electronegativity equalization method in molecular mechanics and molecular dynamics. J Chem Soc Faraday Trans, 1996, 92: 2469－2474
39 Yang Z Z, Wang C S. Atom-bond electronegativity equalization method. 1. Calculation of the charge distribution in large molecules. J Phys Chem A, 1997, 101: 6315－6321
40 Wang C S, Yang Z Z. Atom-bond electronegativity equalization method. II. Lone-pair electron model. J Chem Phys, 1999, 110: 6189－6197
41 Yang Z Z, Wang C S. Atom-bond electronegativity equalization method and its applications based on density functional theory. J Theor Comput Chem, 2003, 2: 273－299
42 Yang Z Z, Cui B Q. Atomic charge calculation of metallobiomolecules in terms of the ABEEM method. J Chem Theory Comput, 2007, 3: 1561－1568
43 Berendsen H J C, Postma J P M, van Gunsteren W F, DiNola A, Haak J R. Ionization potentials of polyacene molecules in micellar systems or in liquid homogeneous solutions. J Chem Phys, 1984, 81: 3684－3689
44 Steinbach P J, Brooks B R. New spherical-cutoff methods for long-range forces in macromolecular simulation. J Comput Chem, 1994, 15: 667－683
45 Hynes J T, Baer M, eds. The Theory of Chemical Reaction Dynamics, Chemical Rubber, Vol. IV, Boca Raton, FL, 1985. 171
46 Carter E A, Cicotti G, Hynes J T, Kapral R. Constrained reaction coordinate dynamics for the simulation of rare events. Chem Phys Lett, 1989, 156: 472－477